Charmed and bottom baryons from lattice nonrelativistic QCD

Nilmani Mathur
TRIUMF, 4004 Wesbrook Mall, Vancouver, British Columbia, Canada V6T 2A3
and Department of Physics and Astronomy, University of Kentucky, Lexington, Kentucky 40506-0055

Randy Lewis
Department of Physics, University of Regina, Regina, Saskatchewan, Canada S4S 0A2

R. M. Woloshyn
TRIUMF, 4004 Wesbrook Mall, Vancouver, British Columbia, Canada V6T 2A3
(Received 1 April 2002; published 29 July 2002)

The mass spectrum of charmed and bottom baryons is computed on anisotropic lattices using quenched lattice nonrelativistic QCD. The masses are extracted by using mass splittings which are more accurate than masses obtained directly by using the nonrelativistic mass-energy relation. Of particular interest are the mass splittings between spin-1/2 and spin-3/2 heavy baryons, and we find that these color hyperfine effects are not suppressed in the baryon sector although they are known to be suppressed in the meson sector. The results are compared with those obtained in a previous nonrelativistic QCD calculation and with those obtained from a Dirac-Wilson action of the D234 type.

DOI: 10.1103/PhysRevD.66.014502 PACS number(s): 12.38.Gc, 14.20.Lq

I. INTRODUCTION

A comprehensive knowledge of the mass spectrum and spin splittings of heavy baryons is important for our understanding of quantum chromodynamics. However, except for singly heavy charmed baryons and only one singly heavy bottom baryon (Λ_b), most of the heavy baryon masses have not yet been measured experimentally [1]. On the theoretical side there are many results on heavy baryon masses from different models, including, for example, a number of quark model variations [2–4].

Using lattice QCD, substantial work has been done in the heavy meson sector. However, so far only very few results have been reported for heavy baryons [5–8], and there is only one work [6] in which heavy (bottom) quarks are treated nonrelativistically. A further study of charmed and bottom heavy baryons on the lattice using nonrelativistic QCD (NRQCD) therefore seems worthwhile.

The extraction of the experimentally observed mass splittings between vector and pseudoscalar mesons remains a challenging problem in lattice QCD; quenched calculations have so far been unable to extract the observed mass splittings [9], and unquenched studies have not resolved the issue [10]. Therefore, it is natural to ask whether lattice results for baryon mass splittings also exhibit a similar suppression compared to experiment.

Empirically, spin splittings in baryons are smaller than those in the meson sector. Moreover, in a lattice simulation the correlators for baryons, particularly for spin-3/2 states, are noisier than those for mesons, and thus, by using lattice QCD, it is comparatively difficult to extract a reliable mass spectrum for heavy baryons. In this work we report on the charmed and bottom baryon mass spectrum and mass splittings by using a nonrelativistic heavy quark action and an improved light quark action on anisotropic lattices.

In Sec. II we summarize different charmed and bottom heavy baryons with their relevant quantum numbers and discuss our choice for interpolating fields. Section III presents the details of the numerical simulation. For heavy quarks, we use the nonrelativistic action from Ref. [11], while a tadpole improved gauge action and an improved Dirac-Wilson action of the D234 type [12] are used for light quarks. Since these actions were previously detailed elsewhere [7,8], we will describe them only in an Appendix. The calculations are done on two different anisotropic lattices with the same gauge configurations as those used in Ref. [8] at $\beta=2.1$ and $\beta=2.3$.

In Sec. IV we present our results. Masses are calculated using two methods: the first uses the standard NRQCD relation between mass and energy while the second employs mass splittings to calculate masses. As mass splittings can be estimated more accurately than masses, errors in the second method are smaller than those obtained in the first. The overall systematic uncertainty is estimated by including scale uncertainty, uncertainty due to the choice of a time window for fitting correlation functions, error due to extrapolation to the physical light quark masses, uncertainty in fixing charm and bottom masses, and uncertainty from our determination of the lattice anisotropy.

Spin splittings are discussed in Sec. V. From our results, along with other published results, we conclude that the suppression of mass splittings is *not present* in the baryon sector in the same way as it is in the meson sector. Over the whole mass range where data are available, quenched lattice QCD simulations yield mass differences between spin-3/2 and spin-1/2 baryons that are comparable to or larger than experimental values.

II. CHARMED AND BOTTOM BARYONS

Singly and doubly charmed and bottom baryons are summarized in Tables I and II, respectively. Table II also includes

TABLE I. Summary of singly heavy baryons, showing valence quark content ($q \equiv u,d$ and $Q \equiv c,b$), spin parity, isospin, and mass (in GeV). The quantity s_l is the total spin of the light quark pair. The experimental values are from Ref. [1].

Baryons	Quark content	J^P	I	s_l	Mass(c)	Mass(b)
Λ_Q	udQ	$\frac{1}{2}^+$	0	0	2.285(1)	5.624(9)
Ξ_Q	qsQ	$\frac{1}{2}^+$	$\frac{1}{2}$	0	2.468(2)	
Σ_Q	qqQ	$\frac{1}{2}^+$	1	1	2.453(1)	
Ξ'_Q	qsQ	$\frac{1}{2}^+$	$\frac{1}{2}$	1	2.575(3)	
Ω_Q	ssQ	$\frac{1}{2}^+$	0	1	2.704(4)	
Σ^*_Q	qqQ	$\frac{3}{2}^+$	1	1	2.518(2)	
Ξ^*_Q	qsQ	$\frac{3}{2}^+$	$\frac{1}{2}$	1	2.645(2)	
Ω^*_Q	ssQ	$\frac{3}{2}^+$	0	1		

doubly heavy states containing two different heavy quarks (charmed and bottom quarks together). The quark content, the spin parity J^P, the isospin I, and s_l, which identifies the total spin of the light quarks (also the spin-flavor symmetry: $s_l=0$ is symmetric while $s_l=1$ is antisymmetric), are shown. Notice that masses for many singly heavy states are not measured yet and there are no data at all on masses for doubly heavy states.

To project out heavy baryon states we use the same interpolating operators as were used in Ref. [8]. For Σ-like baryons we choose

$$\Sigma: \ \epsilon^{abc}[q_a^T C\gamma_5 Q_b]q_c \tag{1}$$

where q is a light quark field and Q is a heavy quark field. Here a,b,c are color indices whereas Dirac indices have been suppressed. For Σ_Q, q is u or d and for Ω_Q, q is s. For doubly heavy Σ-like baryons with equal heavy masses, we interchange the role of light and heavy fields, i.e., to get Ξ_{QQ}, we change $q \to Q$ and $Q \to u$ or d. Similarly, for Ω_{QQ}, the change is $q \to Q, Q \to s$.

TABLE II. Summary of doubly heavy baryons, showing valence quark content ($q \equiv u,d$ and $Q \equiv c,b$), spin parity, isospin, and S_{QQ}, the total spin of the heavy quark pair.

Baryons	Quark content	J^P	I	S_{QQ}
Ξ_{QQ}	qQQ	$\frac{1}{2}^+$	$\frac{1}{2}$	1
Ω_{QQ}	sQQ	$\frac{1}{2}^+$	0	1
Ξ^*_{QQ}	qQQ	$\frac{3}{2}^+$	$\frac{1}{2}$	1
Ω^*_{QQ}	sQQ	$\frac{3}{2}^+$	0	1
Ξ_{bc}	qbc	$\frac{1}{2}^+$	$\frac{1}{2}$	0
Ω_{bc}	sbc	$\frac{1}{2}^+$	0	0
Ξ'_{bc}	qbc	$\frac{1}{2}^+$	$\frac{1}{2}$	1
Ω'_{bc}	sbc	$\frac{1}{2}^+$	0	1
Ξ^*_{bc}	qbc	$\frac{3}{2}^+$	$\frac{1}{2}$	1
Ω^*_{bc}	sbc	$\frac{3}{2}^+$	0	1

The Ξ'_Q is Σ-like but it contains two different light flavors so it is considered separately as

$$\Xi': \ \frac{1}{\sqrt{2}}\{\epsilon^{abc}[q_a'^T C\gamma_5 Q_b]q_c + \epsilon^{abc}[q_a^T C\gamma_5 Q_b]q_c'\}, \tag{2}$$

with $q=u$ or d and $q'=s$.

The Λ-like baryons involve three distinct flavors. A simple choice is the *heavy lambda*:

$$\Lambda: \ \epsilon^{abc}[q_a^T C\gamma_5 q_b']Q_c, \tag{3}$$

where, for Λ_Q, $q=u$, $q'=d$, and for Ξ_Q, $q=u$, $q'=$s. A more symmetrical choice would be the *octet lambda*:

$$\Lambda_o: \ \frac{1}{\sqrt{6}}\epsilon^{abc}\{2[q_a^T C\gamma_5 q_b']Q_c + [q_a^T C\gamma_5 Q_b]q_c' - [q_a'^T C\gamma_5 Q_b]q_c\}, \tag{4}$$

with the same flavor assignment as for the heavy lambda. One can use either of these Λ states as they give consistent results [8]. We choose the octet lambda (Λ_o) for this work. For spin-3/2 baryons we choose the following interpolating field:

$$\Sigma^*: \ \epsilon^{abc}[q_a^T C\gamma_\mu q_b']Q_c, \tag{5}$$

where, for Σ^*_Q, $q=q'$ is u or d and for Ω^*_Q, $q=q'$ is s. To get Ξ^*_Q, one needs to consider $q=u$ or d and $q'=s$. Similarly, to get the doubly heavy states with equal heavy masses one needs to interchange the roles of light and heavy fields. For example, to get Σ^*_{QQ}, one needs to change $q,q' \to Q$ and $Q \to u$ or d, whereas Ω^*_Q requires $q,q' \to Q$ and $Q \to s$.

The operator in Eq. (5) has both spin-1/2 and spin-3/2 states. At zero momentum the corresponding correlation function can be written as [13]

$$C_{ij}(t) = \left(\delta_{ij} - \frac{1}{3}\gamma_i\gamma_j\right)C_{3/2}(t) + \frac{1}{3}\gamma_i\gamma_j C_{1/2}(t), \tag{6}$$

where the i,j's are spatial Lorentz indices and $C_{3/2(1/2)}$ are the spin projections for spin-3/2 (-1/2) states. By choosing different Lorentz components the spin-3/2 part, $C_{3/2}(t)$, is extracted and used to calculate the mass of the spin-3/2 baryons.

Operators for baryons with two unlike heavy flavors may be constructed from the above interpolating operators by interchanging the roles of heavy and light fields. For example, $\Xi^*_{QQ'}$ and $\Omega^*_{QQ'}$ can be obtained from Eq. (5) by letting q, $q' \to Q, Q'$ and $Q \to q$ with $q=u$ or d and $q=s$, respectively. For $\Xi'_{QQ'}$ and $\Omega'_{QQ'}$ we use the symmetrical form again, as given by Eq. (3), making the same replacements, i.e., q, q'

TABLE III. Summary of lattice parameters. The quantity a_t^{-1} is the inverse of the temporal lattice spacing while u_s and u_t are the tadpole improvement factors for spatial and temporal links, respectively.

β	Size	Configurations	a_t^{-1} (GeV)	u_s	u_t
2.1	$12^3\times 32$	720	1.803(42)	0.7858	0.9472
2.3	$14^3\times 38$	442	2.210(72)	0.8040	0.9525

TABLE IV. Hopping parameters and bare masses. Four κ values were used in simulations at each β. κ_s is the hopping parameter for the strange quark, and c and b are the charmed and bottom bare masses, respectively.

β	κ	$\kappa_s(\phi)$	Bare mass	
			c	b
2.1	0.229,0.233,0.237,0.240	0.2338	1.2,1.5	5.0,6.0
2.3	0.229,0.233,0.237,0.240	0.2371	1.04,1.24	3.7,4.2

$\rightarrow Q,Q'$ and $Q\rightarrow q$ with $q=u$ or d and $q=s$, respectively. Finally, $\Xi_{QQ'}$ and $\Omega_{QQ'}$ are the doubly heavy analogues of Λ and they can be obtained from Eqs. (3) and (4) as previously.

III. NUMERICAL SIMULATION

A. Actions

The gauge action as well as the heavy quark NRQCD action used for this work are described in detail in Ref. [11]. The gauge action is tadpole improved and the leading classical error is quartic in lattice spacing. The Hamiltonian corresponding to the NRQCD action is complete to $\mathcal{O}(1/M^3)$ in the classical continuum limit. For light quarks we use a Dirac-Wilson action of the D234 type [12], which has been used previously and detailed in Refs. [7,8]. Its leading classical errors are cubic in lattice spacing. All these actions are summarized in the Appendix.

B. Simulation details

This work is done with two sets of quenched gauge configurations (at $\beta=2.1$ and 2.3) on anisotropic lattices with a bare aspect ratio $a_s/a_t=2$, where the spatial lattice spacing varies from about 0.22 to 0.15 fm.

The renormalized anisotropy is obtained from

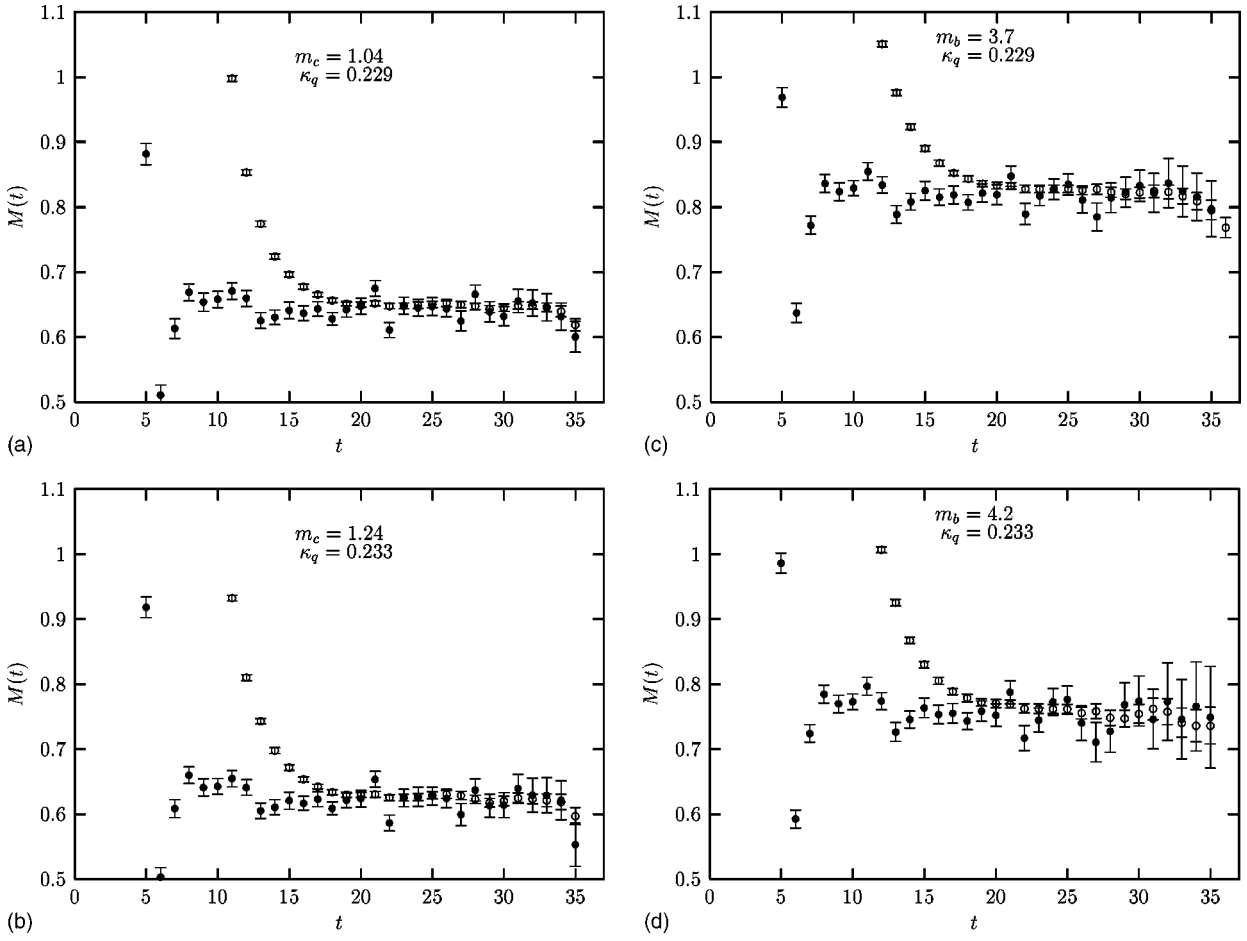

FIG. 1. Effective mass $M(t)$ versus t for singly heavy Σ-like baryons for different combinations of light and heavy quark mass (denoted by hopping parameter κ and bare mass m, respectively). Open symbols are for calculations with a correlation function with local source and sink; filled symbols are for local source and smeared sink.

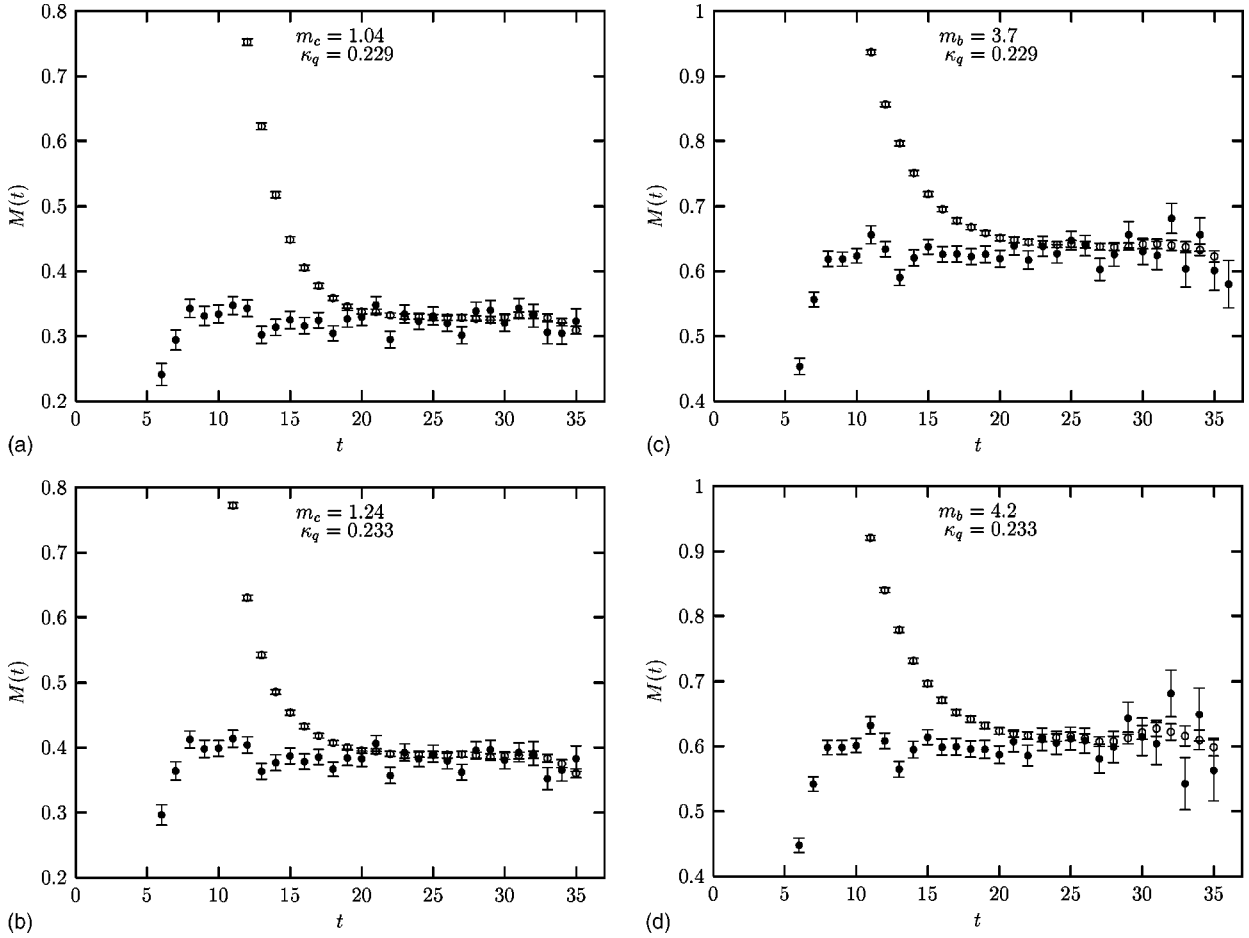

FIG. 2. Effective mass $M(t)$ versus t for doubly heavy Σ-like baryons for different combinations of light and heavy quark mass (denoted by hopping parameter κ and bare mass m, respectively). Open symbols are for calculations with a correlation function with local source and sink; filled symbols are for local source and smeared sink.

$$\xi = \frac{a_s}{a_t} = \frac{a_s V(r_2) - a_s V(r_1)}{a_t V(r_2) - a_t V(r_1)}, \tag{7}$$

where $V(r)$ is the potential between a static quark-antiquark pair with separation r, and is extracted from an exponential fit to a sequence of Wilson loops. In the numerator of Eq. (7) the sequence of Wilson loops extends in a coarsely spaced direction, and in the denominator the sequence extends in the finely spaced direction. The separation r may be along a lattice axis or off axis, and various possibilities were included in the calculation. However, the separation r never includes the finely spaced direction, so that $V(r)$ itself is independent of a_s/a_t. It is convenient to avoid using the largest values of r, where the exponential fit becomes noisier and the periodicity of the lattice can affect a determination of the anisotropy. Our results are

$$\xi = \frac{a_s}{a_t} = \begin{cases} 1.96(2) & \text{for } \beta = 2.1, \\ 1.99(3) & \text{for } \beta = 2.3. \end{cases} \tag{8}$$

We used fixed time boundaries to construct quark propagators, and gauge fields were generated using a pseudo-heat-bath Monte Carlo algorithm with 400 ($\beta = 2.1$) to 800 ($\beta = 2.3$) sweeps between saved configurations. For $\beta = 2.1$, we use 720 configurations and for $\beta = 2.3$ the number of configurations is 442. Two sets of bare masses are used for each heavy quark while four sets of hopping parameters are used for the light one. Bare masses for heavy quarks are chosen to surround the physical value so that an interpolation can be used. For example, at $\beta = 2.1$, the charm mass is between 1.2 and 1.5 and the bottom mass is between 5.0 and 6.0. The charm mass is fixed by setting the η_c mass to its experimental value, whereas the B^0 mass is used to fix the bottom mass. The hopping parameter corresponding to the strange quark is fixed from the D_s meson mass. The temporal lattice spacing and correspondingly the scale is fixed by setting the ρ-meson mass to its experimental value. Summaries of lattice parameters as well as hopping parameters for heavy and light fields are given in Tables III and IV, respectively.

Correlation functions are calculated using interpolating operators in local form at both source and sink. In addition to that we use a gauge invariant smearing for quark propagators at the sink using the smearing function from Eq. (13) of Ref. [14]. These local and sink-smeared correlators are fitted simultaneously to obtain hadron masses. The required correlations among different quantities are taken into account by covariant matrices obtained from singular value decomposition, and the statistical error is estimated from bootstrapping

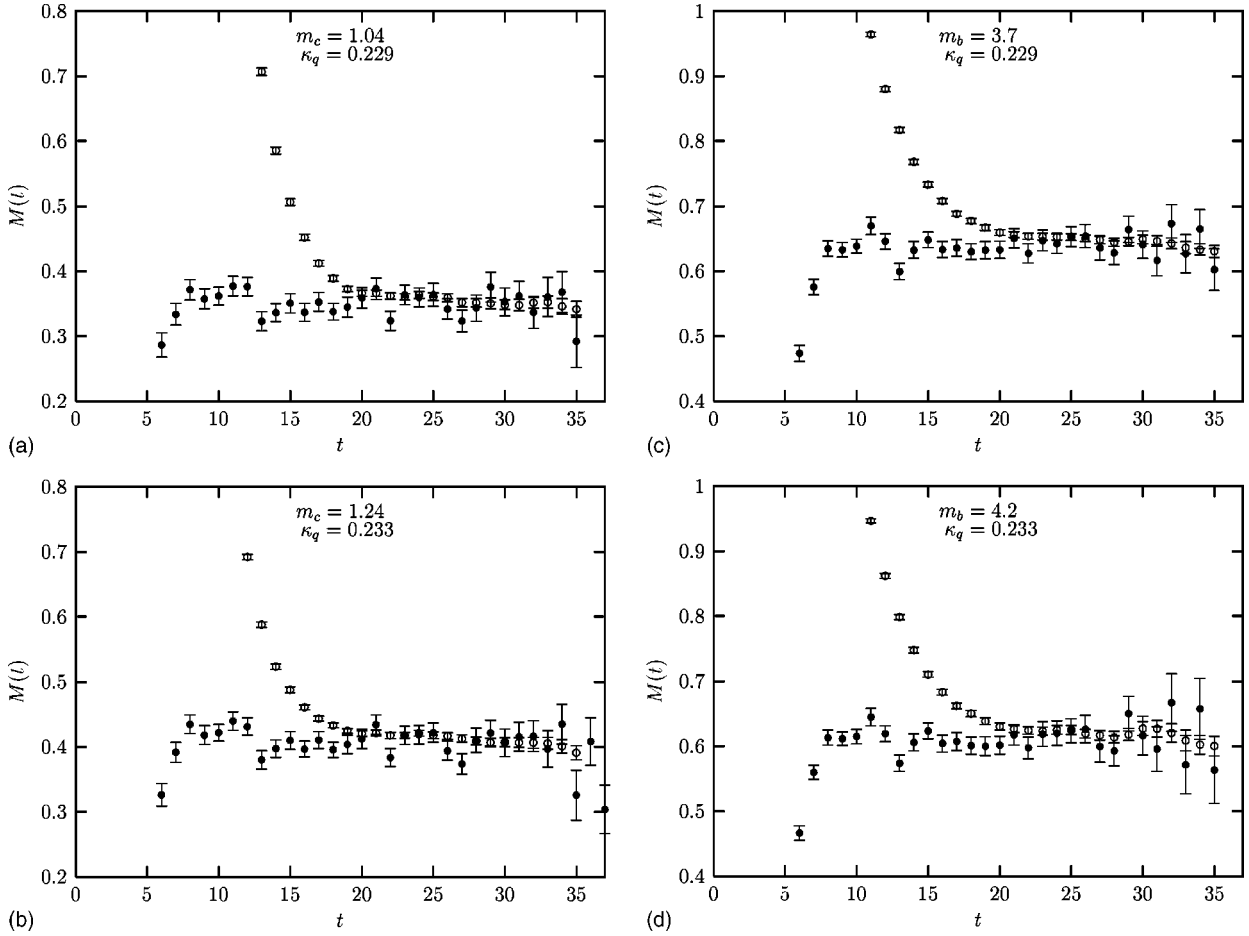

FIG. 3. Effective mass $M(t)$ versus t for doubly heavy Σ^*-like baryons for different combinations of light and heavy quark mass (denoted by hopping parameter κ and bare mass m, respectively). Open symbols are for calculations with a correlation function with local source and sink; filled symbols are for local source and smeared sink.

the fitting procedure. As in Ref. [8], local correlators are fitted with two exponential functions $[A\exp(-m_1x)+B\exp(-m_2x)]$, while the sink-smeared correlation function is fitted with a single exponential $[C\exp(-m_1x)]$. The mass parameter for the sink-smeared fit is constrained to be the same as the lowest mass of the fit to the local correlator. The time window for the fit is chosen in such a way that the ending time is large and the fit is stable under variation of both starting and ending time by a few time steps. Light quark extrapolation is done by extrapolating the hadron masses extracted at four light quark masses with the form $c_0+c_2m_\pi^2+c_3m_\pi^3$, where m_π is the pion mass. In most of the cases the cubic (m_π^3) contributions are small and they are included only to get systematic errors.

Figures 1–3 show some representative examples of our simulation results. We plot the effective mass for different heavy baryons versus time t, where the effective mass is defined to be $M(t)=\ln[g(t)/g(t+1)]$ with $g(t)$ being the zero-momentum time correlation function of baryon fields. Open symbols in these figures are for calculations with a correlation function with local source and sink; filled symbols are for local source and smeared sink. There is good agreement between local and smeared results at large times.

It should be noted that the actual fits to determine the masses are performed directly with the correlation functions, and not on the effective masses plotted in Figs. 1–3, but the plots provide an indication of the quality of our data. Although the sink-smeared results appear to be somewhat noisy, they are quite helpful in constraining the two-exponential fit of the local correlation function.

C. Mass extraction

The kinetic mass of a nonrelativistic state can be extracted from the usual NRQCD relation [11]

$$M_{kin}=\frac{2\pi^2}{N_s^2\xi^2 a_t[a_t(E_p-E_0)]}, \tag{9}$$

which is derived from $E=p^2/2M_{kin}$. Here $N=La_s$, with L being the lattice size and a_s the spatial lattice spacing. $\xi=a_t/a_s$ is the anisotropy whereas E_0 and E_p are simulation energies corresponding to the ground state and the state with momentum $p=2\pi/La_s$, respectively. Mass differences between two states (H_1 and H_2) with the same heavy quark can be obtained by taking the difference of their zero-momentum simulation energies:

$$M_{H_1} - M_{H_2} = E^1_{sim}(0) - E^2_{sim}(0), \quad (10)$$

which follows from the lattice NRQCD expression for the hadron mass

$$M_H = E_{sim}(0) + ZM_Q - E_{shift}, \quad (11)$$

where E_{sim} is the simulation energy at zero momentum and the last two terms represent the renormalized heavy quark mass. The bare quark mass M_Q has both a multiplicative (Z) and additive (E_{shift}) renormalization [15], which should be independent of the hadronic state. A more precise result is obtained for heavy hadron masses with the heaviest light quark ($\kappa = 0.229$) rather than with a lighter light quark ($\kappa = 0.233$ and higher).

Moreover, mass differences [Eq. (10)] can be calculated more precisely than masses [Eq. (9)]. Therefore, for example, one can calculate a meson mass from the relation

$$M(q_l, Q) = M(q_h, H) - \Delta M = M(q_h, H) - \Delta E, \quad (12)$$

where

$$\Delta M = \Delta E = E(q_h, Q) - E(q_l, Q). \quad (13)$$

Here q_h and q_l denote the heaviest light quark and a lighter one, respectively, and $M(q_h, H)$ is extracted by using Eq. (9). Equation (13) is valid as long as Z in Eq. (11) is the same, i.e., both states consist of the same heavy quark Q.

Similarly, masses of singly and doubly heavy baryons can be extracted from meson masses by using

$$M(q_1 q_2, Q) = M(q_h, Q) - \Delta E_{sh}, \quad (14)$$

$$M(q_1, QQ) = M(QQ) - \Delta E_{dh}, \quad (15)$$

where

$$E_{sh} = E(q_h, Q) - E(q_1 q_2, Q), \quad (16)$$

$$E_{dh} = E(QQ) - E(q_1, QQ). \quad (17)$$

For example, the $\Sigma_{c(b)}$ mass is extracted by taking its difference (at each κ) from the D (B^0) mass (m) at $\kappa = 0.229$ and then subtracting that from m. Masses extracted by using Eq. (9) and Eqs. (12)–(17) are consistent with each other. However, errors in the second method are smaller than in the previous one.

IV. RESULTS

The mass spectrum and spin splittings of heavy quark baryons have been computed on an anisotropic lattice using the NRQCD heavy quark action. The results are summarized in Table V, where the first error is the statistical error obtained from a bootstrap analysis with a bootstrap sample size equal to the configuration sample size. The second error is an overall systematic error due to scale and anisotropy uncertainties, the uncertainty due to choosing a time window, the light quark extrapolation error, and the strange quark mass uncertainty. Mesons, singly heavy baryons, and doubly heavy baryons are separated into different groups by horizontal lines. In Table VI we compare our results with those obtained by using a relativistic (D234) heavy quark action [8] and experimental numbers (where available). One can see that the NRQCD results and D234 results are consistent with each other. The results are also consistent with a previous NRQCD calculation [6]. As in Ref. [8], it is found that the suppression of spin splittings is not present in the baryon

TABLE V. Results for meson and baryon masses and mass splittings (in MeV) calculated using the NRQCD action for charm (c) and bottom (b) quarks. The first error is statistical while the second error comprises systematic errors due to scale, time window, and anisotropy. Rows are separated into mesons, singly heavy charmed baryons, doubly heavy charmed baryons, singly heavy bottom baryons, and doubly heavy bottom baryons, respectively.

	$\beta = 2.1$	$\beta = 2.3$
$J/\Psi - \eta_c$	$70(2)(^{5}_{4})$	$76(3)(^{7}_{5})$
D	$1842(28)(^{33}_{31})$	$1850(35)(^{28}_{24})$
D_s	$1980(23)(^{26}_{23})$	$1958(33)(^{23}_{21})$
$D^* - D$	$98(6)(^{5}_{3})$	$101(6)(^{6}_{5})$
$D_s^* - D_s$	$94(4)(^{4}_{3})$	$96(4)(^{4}_{5})$
B_s^0	$5380(108)(^{21}_{18})$	$5375(103)(^{20}_{21})$
$B^* - B^0$	$32(4)(^{3}_{2})$	$35(6)(^{3}_{3})$
$B_s^* - B_s^0$	$29(3)(^{2}_{2})$	$32(4)(^{3}_{2})$
Σ_c	$2407(32)(^{32}_{37})$	$2452(38)(^{38}_{36})$
Ξ_c	$2440(27)(^{28}_{26})$	$2473(34)(^{34}_{33})$
Ω_c	$2652(25)(^{27}_{31})$	$2678(33)(^{33}_{31})$
$\Sigma_c^* - \Sigma_c$	$75(20)(^{14}_{12})$	$86(18)(^{12}_{13})$
$\Xi_c^* - \Xi_c'$	$71(18)(^{12}_{9})$	$81(16)(^{11}_{10})$
$\Omega_c^* - \Omega_c$	$65(13)(^{7}_{8})$	$74(14)(^{8}_{8})$
$\Sigma_c - \Lambda_c$	$128(28)(^{39}_{28})$	$162(36)(^{33}_{26})$
$\Xi_c' - \Xi_c$	$104(19)(^{20}_{23})$	$126(21)(^{15}_{22})$
Ξ_{cc}	$3562(47)(^{27}_{25})$	$3588(66)(^{32}_{27})$
Ω_{cc}	$3681(44)(^{17}_{19})$	$3698(60)(^{26}_{23})$
$\Xi_{cc}^* - \Xi_{cc}$	$63(14)(^{9}_{7})$	$70(11)(^{7}_{7})$
$\Omega_{cc}^* - \Omega_{cc}$	$56(8)(^{7}_{6})$	$63(7)(^{5}_{5})$
Λ_b	$5664(98)(^{33}_{46})$	$5672(102)(^{35}_{41})$
Ξ_b	$5762(83)(^{29}_{38})$	$5788(86)(^{30}_{36})$
Ω_b	$6021(75)(^{27}_{34})$	$6040(77)(^{25}_{31})$
$\Sigma_b^* - \Sigma_b$	$22(10)(^{7}_{6})$	$24(11)(^{7}_{5})$
$\Xi_b^* - \Xi_b'$	$21(10)(^{7}_{6})$	$23(11)(^{7}_{5})$
$\Omega_b^* - \Omega_b$	$18(7)(^{6}_{4})$	$20(8)(^{5}_{3})$
$\Sigma_b - \Lambda_b$	$141(24)(^{30}_{22})$	$175(27)(^{26}_{24})$
$\Xi_b' - \Xi_b$	$124(22)(^{32}_{18})$	$148(25)(^{24}_{15})$
$\Xi_{bb}^* - \Xi_{bb}$	$22(6)(^{4}_{3})$	$20(6)(^{3}_{4})$
$\Omega_{bb}^* - \Omega_{bb}$	$20(4)(^{3}_{3})$	$19(4)(^{3}_{3})$
Ξ_{cb}'	$6810(150)(^{62}_{79})$	$6840(228)(^{58}_{72})$
Ω_{cb}'	$6935(135)(^{75}_{89})$	$6954(214)(^{62}_{81})$
$\Xi_{cb}^* - \Xi_{cb}'$	$46(8)(^{4}_{6})$	$43(9)(^{6}_{6})$
$\Omega_{cb}^* - \Omega_{cb}'$	$40(6)(^{4}_{5})$	$39(6)(^{5}_{5})$
$\Xi_{cb} - \Xi_{cb}'$	$11(6)(^{4}_{5})$	$9(5)(^{6}_{4})$
$\Omega_{cb} - \Omega_{cb}'$	$10(5)(^{4}_{4})$	$9(4)(^{4}_{4})$

TABLE VI. Results for charmed baryon masses and mass differences (in MeV) compared to experimental values. The first row of lattice results (taken from [8]) were calculated using a relativistic action of the D234 type for the charmed quark while for the second row (this work) the NRQCD action was used.

	Lattice results			Expt.
	$\beta=2.1$	$\beta=2.3$	$\beta=2.5$	
Σ_c	$2379(31)(^{23}_{18})$	$2490(14)(^{17}_{33})$	$2493(22)(^{21}_{29})$	2455
	$2407(32)(^{32}_{37})$	$2452(38)(^{38}_{36})$		
Ξ_c	$2455(17)(^{11}_{42})$	$2462(14)(^{5}_{30})$	$2481(14)(^{1}_{34})$	2468
	$2440(27)(^{28}_{26})$	$2473(34)(^{34}_{33})$		
Ω_c	$2671(11)(^{11}_{59})$	$2699(10)(^{8}_{41})$	$2700(11)(^{8}_{40})$	2704
	$2652(25)(^{27}_{31})$	$2678(33)(^{33}_{31})$		
$\Sigma_c^*-\Sigma_c$	$62(33)(^{19}_{32})$	$82(12)(^{9}_{6})$	$76(19)(^{15}_{4})$	64
	$75(20)(^{14}_{12})$	$86(18)(^{12}_{13})$		
$\Xi_c^*-\Xi_c'$	$52(15)(^{8}_{4})$	$82(10)(^{8}_{5})$	$77(9)(^{7}_{5})$	70
	$71(18)(^{12}_{9})$	$81(16)(^{11}_{10})$		
$\Omega_c^*-\Omega_c$	$50(17)(^{11}_{6})$	$73(8)(^{7}_{5})$	$69(7)(^{5}_{6})$	
	$65(13)(^{7}_{8})$	$74(14)(^{8}_{8})$		
Ξ_{cc}	$3608(15)(^{13}_{35})$	$3595(12)(^{21}_{22})$	$3605(12)(^{23}_{19})$	
	$3562(47)(^{27}_{25})$	$3588(66)(^{32}_{27})$		
Ω_{cc}	$3747(9)(^{11}_{47})$	$3727(9)(^{16}_{40})$	$3733(9)(^{7}_{38})$	
	$3681(44)(^{17}_{19})$	$3698(60)(^{26}_{23})$		
$\Xi_{cc}^*-\Xi_{cc}$	$58(14)(^{16}_{10})$	$83(8)(^{7}_{10})$	$80(10)(^{3}_{7})$	
	$63(14)(^{9}_{7})$	$70(11)(^{7}_{7})$		
$\Omega_{cc}^*-\Omega_{cc}$	$57(8)(^{10}_{9})$	$72(5)(^{4}_{5})$	$68(5)(^{6}_{5})$	
	$56(8)(^{7}_{6})$	$63(7)(^{5}_{5})$		

sector, although such a suppression is known to be characteristic of the heavy meson sector. One can also see that the spin splittings for doubly heavy baryons are as large as their singly heavy counterparts.

V. DISCUSSION AND SUMMARY

In order to put the results of the present calculation into perspective it is useful to consider spin splittings over the whole range of available quark masses. We start with mesons where it has been known for a long time that the squared mass difference $M_V^2-M_P^2$ for vector and pseudoscalar mesons is approximately constant for all mesons of the form $Q\overline{q}$, where q is up or down and Q is any light or heavy flavor. This relation is illustrated in Fig. 4 for the mass pairs (ρ,π), (K^*,K), (D^*,D), and (B^*,B). Also shown are the results of lattice simulations including the present work. The tendency for quenched lattice QCD to underestimate the spin splittings relative to experimental values is clearly visible.

In Ref. [8] we showed that it is useful to consider the behavior of the spin splittings in the baryon sector as a function of quark mass also in terms of the mesonic average mass $(M_V+M_P)/2$. The results for the baryon pairs (Δ,N), (Σ^*,Σ), (Σ_c^*,Σ_c), and (Σ_b^*,Σ_b) are shown in Fig. 5. It is a remarkable empirical fact that the baryon spin splitting scales almost exactly like the inverse of the average meson mass. The implication is that the ratio of meson to baryon spin splittings is almost constant. This was discussed in Ref. [8] and was to some extent anticipated by Lipkin [18] from the point of view of the quark model (see also Lipkin and O'Donnell [19]).

The results of quenched lattice calculations are also shown in Fig. 5. The suppression of spin splittings relative to experiment, visible for mesons, is not seen for baryons. The results of the present lattice NRQCD calculation support this conclusion in the charm and bottom sectors. It is clear that a definitive measurement of Σ_b and Σ_b^* masses would be

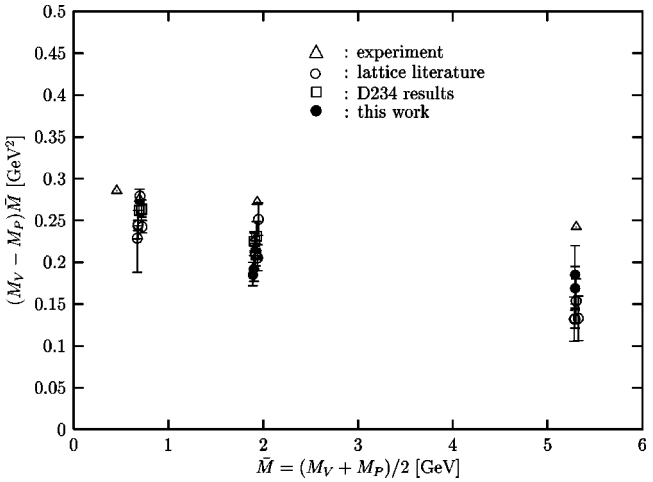

FIG. 4. Spin splittings in the meson sector, plotted as $(M_V-M_P)\bar{M}$ versus $\bar{M}$ where $\bar{M}$ is the average vector and pseudoscalar meson mass $(M_V+M_P)/2$. "Lattice literature" results are from Refs. [11,16,17] while D234 results are from Ref. [8].

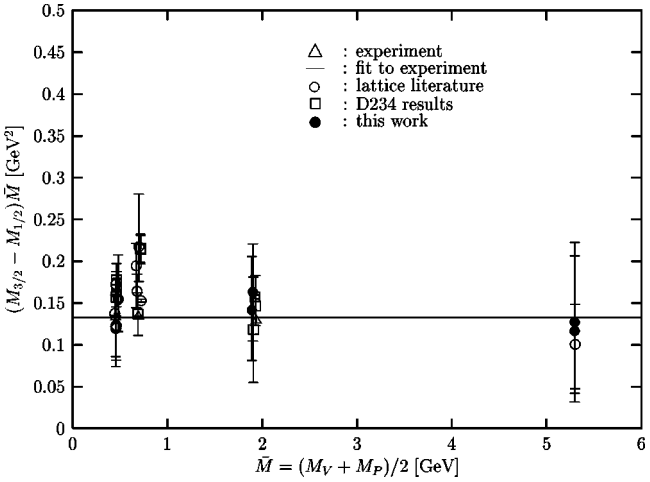

FIG. 5. Spin splittings in the baryon sector plotted as $(M_{3/2}-M_{1/2})\bar{M}$ versus $\bar{M}$ where $\bar{M}$ is the average vector and pseudoscalar meson mass $(M_V+M_P)/2$. "Lattice literature" results are from Ref. [16] while "D234 results" are from Ref. [8]. The solid line is a fit to the experimental data.

highly desirable to extend the experimental comparison to larger mass values.

From the point of view of lattice NRQCD our results present an interesting challenge. As is well known, the spin splittings of both charmonium [20] and heavy-light mesons [9,11] are clearly underestimated by lattice NRQCD simulations. Up to now, these simulations have used couplings modified only by mean-field tadpole factors. It is tempting to speculate that there are additional large perturbative corrections to these couplings. In particular, it might seem that a correction to the quark coupling with the chromomagnetic field [the c_4 term in Eq. (A5)] has the potential to cure the spin splitting deficiency for both charmonium and heavy-light mesons. However, one has to be cautious in wishing for such a cure as it would upset the already reasonable values for spin splittings in the baryon sector.

To summarize, we have calculated the masses of baryons containing one or two heavy quarks using quenched lattice QCD. NRQCD is used to describe charm and bottom quarks. In the charm sector the results of this work are compatible with those obtained previously where a Dirac-Wilson action of the D234 type was used for the heavy quark. No suppression of the spin splittings observed in lattice NRQCD simulations of heavy-light mesons is seen in the heavy baryon sector.

This and our previous work [8] leave a number of difficult open questions. One would like to be able to improve the lattice calculations of baryons to reduce the uncertainties to the same level achievable in mesons. Also how (and whether) the addition of dynamical quarks to the simulations will solve the dilemma of spin splittings has yet to be understood. A phenomenological issue is to understand the remarkable constancy in the meson to baryon spin splitting ratio over the whole available quark mass range. On the experimental side it will be a significant challenge to extend baryon mass measurements in the bottom and doubly heavy sectors.

ACKNOWLEDGMENTS

This work was supported in part by the Natural Sciences and Engineering Research Council of Canada. N.M. is also thankful to CCS of University of Kentucky for its support. Some of the computing was done on hardware funded by the Canada Foundation for Innovation, with contributions from Compaq Canada, Avnet Enterprise Solutions, and the Government of Saskatchewan.

APPENDIX: DETAILS OF ACTIONS

1. NRQCD action

The heavy quark action is nonrelativistic and is discretized to give the following Green's function propagation:

$$G_{\tau+1}=\left(1-\frac{a_t H_B}{2}\right)\left(1-\frac{a_t H_A}{2n}\right)^n U_4^\dagger \left(1-\frac{a_t H_A}{2n}\right)^n \times\left(1-\frac{a_t H_B}{2}\right)G_\tau, \tag{A1}$$

The nonrelativistic Hamiltonian is complete to $O(1/M^3)$ in the classical continuum limit:

$$H=H_0+\delta H, \tag{A2}$$

$$H_0=\frac{-\Delta^{(2)}}{2M}, \tag{A3}$$

$$\delta H=\delta H^{(1)}+\delta H^{(2)}+\delta H^{(3)}+O(1/M^4), \tag{A4}$$

$$\delta H^{(1)}=-\frac{c_4}{u_s^4}\frac{g}{2M}\boldsymbol{\sigma}\cdot\tilde{\mathbf{B}}+c_5\frac{a_s^2\Delta^{(4)}}{24M}, \tag{A5}$$

$$\delta H^{(2)}=\frac{c_2}{u_s^2u_t^2}\frac{ig}{8M^2}(\tilde{\boldsymbol{\Delta}}\cdot\tilde{\mathbf{E}}-\tilde{\mathbf{E}}\cdot\tilde{\boldsymbol{\Delta}}) -\frac{c_3}{u_s^2u_t^2}\frac{g}{8M^2}\boldsymbol{\sigma}\cdot(\tilde{\boldsymbol{\Delta}}\times\tilde{\mathbf{E}}-\tilde{\mathbf{E}}\times\tilde{\boldsymbol{\Delta}})-c_6\frac{a_s(\Delta^{(2)})^2}{16n\xi M^2}, \tag{A6}$$

$$\delta H^{(3)}=-c_1\frac{(\Delta^{(2)})^2}{8M^3}-\frac{c_7}{u_s^4}\frac{g}{8M^3}\{\tilde{\Delta}^{(2)},\boldsymbol{\sigma}\cdot\tilde{\mathbf{B}}\} -\frac{c_9ig^2}{8M^3}\boldsymbol{\sigma}\cdot\left(\frac{\tilde{\mathbf{E}}\times\tilde{\mathbf{E}}}{u_s^4u_t^4}+\frac{\tilde{\mathbf{B}}\times\tilde{\mathbf{B}}}{u_s^8}\right)-\frac{c_{10}g^2}{8M^3}\left(\frac{\tilde{\mathbf{E}}^2}{u_s^4u_t^4}+\frac{\tilde{\mathbf{B}}^2}{u_s^8}\right) -c_{11}\frac{a_s^2(\Delta^{(2)})^3}{192n^2\xi^2M^3}. \tag{A7}$$

Here a tilde signifies that discretization errors have been removed. In particular,

$$\tilde{E}_i = \tilde{F}_{4i}, \tag{A8}$$

$$\tilde{B}_i = \frac{1}{2}\epsilon_{ijk}\tilde{F}_{jk}, \tag{A9}$$

$$\begin{aligned}\tilde{F}_{\mu\nu}(x) = {} & \frac{5}{6}F_{\mu\nu}(x) - \frac{1}{6u_\mu^2}U_\mu(x)F_{\mu\nu}(x+\hat{\mu})U_\mu^\dagger(x) \\ & - \frac{1}{6u_\mu^2}U_\mu^\dagger(x-\hat{\mu})F_{\mu\nu}(x-\hat{\mu})U_\mu(x-\hat{\mu}) \\ & - (\mu \leftrightarrow \nu).\end{aligned} \tag{A10}$$

The various spatial lattice derivatives are defined as follows:

$$a_s\Delta_i G(x) = \frac{1}{2u_s}[U_i(x)G(x+\hat{\imath}) - U_i^\dagger(x-\hat{\imath})G(x-\hat{\imath})], \tag{A11}$$

$$a_s\Delta_i^{(+)}G(x) = \frac{U_i(x)}{u_s}G(x+\hat{\imath}) - G(x), \tag{A12}$$

$$a_s\Delta_i^{(-)}G(x) = G(x) - \frac{U_i^\dagger(x-\hat{\imath})}{u_s}G(x-\hat{\imath}), \tag{A13}$$

$$\begin{aligned}a_s^2\Delta_i^{(2)}G(x) = {} & \frac{U_i(x)}{u_s}G(x+\hat{\imath}) - 2G(x) \\ & + \frac{U_i^\dagger(x-\hat{\imath})}{u_s}G(x-\hat{\imath}),\end{aligned} \tag{A14}$$

$$\tilde{\Delta}_i = \Delta_i - \frac{a_s^2}{6}\Delta_i^{(+)}\Delta_i\Delta_i^{(-)}, \tag{A15}$$

$$\Delta^{(2)} = \sum_i \Delta_i^{(2)}, \tag{A16}$$

$$\tilde{\Delta}^{(2)} = \Delta^{(2)} - \frac{a_s^2}{12}\Delta^{(4)}, \tag{A17}$$

$$\Delta^{(4)} = \sum_i (\Delta_i^{(2)})^2. \tag{A18}$$

2. Gauge field action

The leading classical errors of the gauge field action are quartic in lattice spacing. The action is

$$\begin{aligned}S_G(U) = \frac{5\beta}{3}\Bigg[& \frac{1}{u_s^4\xi}\sum_{\rm ps}\left(1 - \frac{1}{3}\mathrm{Re\,Tr}\,U_{\rm ps}\right) - \frac{1}{20u_s^6\xi} \\ & \times \sum_{\rm rs}\left(1 - \frac{1}{3}\mathrm{Re\,Tr}\,U_{\rm rs}\right) + \frac{\xi}{u_s^2u_t^2} \\ & \times \sum_{\rm pt}\left(1 - \frac{1}{3}\mathrm{Re\,Tr}\,U_{\rm pt}\right) - \frac{\xi}{20u_s^4u_t^2} \\ & \times \sum_{\rm rst}\left(1 - \frac{1}{3}\mathrm{Re\,Tr}\,U_{\rm rst}\right) - \frac{\xi}{20u_s^2u_t^4} \\ & \times \sum_{\rm rts}\left(1 - \frac{1}{3}\mathrm{Re\,Tr}\,U_{\rm rts}\right)\Bigg],\end{aligned} \tag{A19}$$

where the anisotropic ratio $\xi \equiv a_s/a_t$ and β is the lattice gauge field coupling constant. ps indicates spatial plaquettes, rs, spatial planar 1×2 rectangles, pt, plaquettes in the temporal-spatial plane, and rst (rts) rectangles with the long side in a spatial (temporal) direction.

3. Light quark action

For light quarks, we used a D234 action [8,12] with parameters set to their tadpole improved classical values. Its leading classical errors are cubic in lattice spacing and the action can be written as

$$\begin{aligned}S_F(\bar{q},q;U) = {} & \frac{4\kappa}{3}\sum_{x,i}\left[\frac{1}{u_s\xi^2}D_{1i}(x) - \frac{1}{8u_s^2\xi^2}D_{2i}(x)\right] \\ & + \frac{4\kappa}{3}\sum_x\left[\frac{1}{u_t}D_{1t}(x) - \frac{1}{8u_t^2}D_{2t}(x)\right] \\ & + \frac{2\kappa}{3u_s^4\xi^2}\sum_{x,i<j}\bar{\psi}(x)\sigma_{ij}F_{ij}(x)\psi(x) \\ & + \frac{2\kappa}{3u_s^2u_t^2\xi}\sum_{x,i}\bar{\psi}(x)\sigma_{0i}F_{0i}(x)\psi(x) \\ & - \sum_x \bar{\psi}(x)\psi(x),\end{aligned} \tag{A20}$$

where

$$\begin{aligned}D_{1i}(x) = {} & \bar{\psi}(x)(1-\xi\gamma_i)U_i(x)\psi(x+\hat{\imath}) \\ & + \bar{\psi}(x+\hat{\imath})(1+\xi\gamma_i)U_i^\dagger(x)\psi(x),\end{aligned} \tag{A21}$$

$$D_{1t}(x) = \overline{\psi}(x)(1-\gamma_4)U_4(x)\psi(x+\hat{t}) + \overline{\psi}(x+\hat{t})(1+\gamma_4)U_4^\dagger(x)\psi(x), \tag{A22}$$

$$D_{2i}(x) = \overline{\psi}(x)(1-\xi\gamma_i)U_i(x)U_i(x+\hat{i})\psi(x+2\hat{i}) + \overline{\psi}(x+2\hat{i})(1+\xi\gamma_i)U_i^\dagger(x+\hat{i})U_i^\dagger(x)\psi(x), \tag{A23}$$

$$D_{2t}(x) = \overline{\psi}(x)(1-\gamma_4)U_4(x)U_4(x+\hat{t})\psi(x+2\hat{t}) + \overline{\psi}(x+2\hat{t})(1+\gamma_4)U_4^\dagger(x+\hat{t})U_4^\dagger(x)\psi(x), \tag{A24}$$

$$gF_{\mu\nu}(x) = \frac{1}{2i}[\Omega_{\mu\nu}(x) - \Omega_{\mu\nu}^\dagger(x)] - \frac{1}{3}\mathrm{Im}[\mathrm{Tr}\,\Omega_{\mu\nu}(x)], \tag{A25}$$

$$\begin{aligned}\Omega_{\mu\nu} = \frac{-1}{4}[&U_\mu(x)U_\nu(x+\hat{\mu})U_\mu^\dagger(x+\hat{\nu})U_\nu^\dagger(x)\\ &+U_\nu(x)U_\mu^\dagger(x-\hat{\mu}+\hat{\nu})U_\nu^\dagger(x-\hat{\mu})U_\mu(x-\hat{\mu})\\ &+U_\mu^\dagger(x-\hat{\mu})U_\nu^\dagger(x-\hat{\mu}-\hat{\nu})U_\mu(x-\hat{\mu}-\hat{\nu})\\ &\times U_\nu(x-\hat{\nu})+U_\nu^\dagger(x-\hat{\nu})U_\mu(x-\hat{\nu})\\ &\times U_\nu(x+\hat{\mu}-\hat{\nu})U_\mu^\dagger(x)].\end{aligned} \tag{A26}$$

[1] Particle Data Group, D.E. Groom *et al.*, Eur. Phys. J. C **15**, 1 (2000).

[2] S.S. Gershtein, V.V. Kiselev, A.K. Likhoded, and A.I. Onishchenko, Phys. Rev. D **62**, 054021 (2000).

[3] D.U. Matrasulov, M.M. Musakhanov, and T. Morii, Phys. Rev. C **61**, 045204 (2000); D. Ebert *et al.*, Phys. Rev. D (to be published), hep-ph/0201217.

[4] V.V. Kiselev and A.K. Likhoded, hep-ph/0103169; Sheng-Ping Tong, Phys. Rev. D **62**, 054024 (2000); V.V. Kiselev and A.I. Onishchenko, Nucl. Phys. **B581**, 432 (2000).

[5] UKQCD Collaboration, K.C. Bowler *et al.*, Phys. Rev. D **54**, 3619 (1996).

[6] A. Ali Khan *et al.*, Phys. Rev. D **62**, 054505 (2000).

[7] R.M. Woloshyn, Phys. Lett. B **476**, 309 (2000).

[8] R. Lewis, N. Mathur, and R.M. Woloshyn, Phys. Rev. D **64**, 094509 (2001).

[9] For a review, see C. Bernard, Nucl. Phys. B (Proc. Suppl.) **94**, 159 (2001).

[10] C. Stewart and R. Koniuk, Phys. Rev. D **63**, 054503 (2001); CP-PACS Collaboration, T. Manke *et al.*, *ibid.* **62**, 114508 (2000); S. Collins *et al.*, *ibid.* **60**, 074504 (1999).

[11] R. Lewis and R.M. Woloshyn, Phys. Rev. D **62**, 114507 (2000).

[12] M. Alford, T.R. Klassen, and G.P. Lepage, Nucl. Phys. **B496**, 377 (1997).

[13] M. Benmerrouche, R.M. Davidson, and N.C. Mukhopadhyay, Phys. Rev. C **39**, 2339 (1989).

[14] C. Alexandrou, S. Güsken, F. Jegerlehner, K. Schilling, and R. Sommer, Nucl. Phys. **B414**, 815 (1994).

[15] C.T.H. Davies and B.A. Thacker, Phys. Rev. D **45**, 915 (1992).

[16] F. Butler *et al.*, Nucl. Phys. **B430**, 179 (1994); S. Aoki *et al.*, Phys. Rev. Lett. **84**, 238 (2000); A. Ali Khan *et al.*, Phys. Rev. D **62**, 054505 (2000); K.C. Bowler *et al.*, *ibid.* **62**, 054506 (2000).

[17] P. Boyle, Nucl. Phys. B (Proc. Suppl.) **63A-C**, 314 (1998); K.I. Ishikawa *et al.*, Phys. Rev. D **61**, 074501 (2000); J. Hein *et al.*, *ibid.* **62**, 074503 (2000).

[18] H.J. Lipkin, Phys. Lett. B **171**, 293 (1986).

[19] H.J. Lipkin and P.J. O'Donnell, Phys. Lett. B **409**, 412 (1997).

[20] H.D. Trottier, Phys. Rev. D **55**, 6844 (1997); N.H. Shakespeare and H.D. Trottier, *ibid.* **58**, 034502 (1998).